Voltage Clamp Analysis of Embryonic Heart Cell Aggregates

RICHARD D. NATHAN and ROBERT L. DEHAAN

From the Department of Anatomy, Emory University School of Medicine, Atlanta, Georgia 30322. Dr. Nathan's present address is Department of Physiology, Texas Tech University School of Medicine, Lubbock, Texas 79430.

ABSTRACT The double-microelectrode voltage clamp technique was applied to small spheroidal aggregates of heart cells from 7-d chick embryos. A third intracellular electrode was sometimes used to monitor spatial homogeneity. On average, aggregates were found to deviate from isopotentiality by 12% during the first 3–5 ms of large depolarizing voltage steps, when inward current was maximal, and by <3% thereafter. Two components of inward current were recorded: (*a*) a fast, transient current associated with the rapid upstroke of the action potential, which was abolished by tetrodotoxin (TTX); and (*b*) a slower inward current related to the plateau, which was not affected by TTX but was blocked by D600. The magnitudes, kinetics, and voltage dependence of these two inward currents and a delayed outward current were similar to those reported for adult cardiac preparations. From a holding potential of −60 mV, the peak fast component at the point of maximal activation (−20 mV) was −185 μA/cm^2. This value was about seven times greater than the maximal slow component which peaked at 0 mV. The ratio of rate constants for the decay of the two currents was between 10:1 and 30:1.

INTRODUCTION

The voltage clamp technique has been used by numerous investigators to describe the voltage- and time-dependent conductances in cardiac tissue. The main conclusion from these analyses is that the ionic currents that underlie the action potential in the heart are more numerous and complex than in the classic squid axon (for reviews, see Trautwein, 1973; McAllister et al., 1975; Noma and Irisawa, 1976; Beeler and Reuter, 1977; Trautwein and McDonald, 1978).

A major problem in the quantitative interpretation of voltage clamp data in heart tissue arises out of the multicellular nature of the preparation. Heart muscle is composed of individual cells connected by junctions of low but varying resistance, into fibers of complex geometry (DeHaan and Fozzard, 1975; Kensler et al., 1977). Substantial voltage gradients may exist within such fibers, and currents crossing the membrane of one cell may differ from those flowing in a distant cell. The problem of electrical inhomogeneity of cardiac tissue and the limitations it places on voltage clamp analyses have been documented and discussed at length. It is generally agreed that, because of the multicellular nature of heart muscle, it has not been possible to control ideally the membrane potential of any preparation. Thus, there remain substantial uncertainties

J. GEN. PHYSIOL. © The Rockefeller University Press · 0022-1295/79/02/0175-24$1.00
Volume 73 February 1979 175–198

regarding the absolute magnitude, kinetics, and voltage dependence of the various action currents (Johnson and Lieberman, 1971; Fozzard and Beeler, 1975; Ramón et al., 1975; Attwell and Cohen, 1977).

Nevertheless, an understanding of the ionic currents in cardiac muscle is beginning to emerge from application of the voltage clamp. The action potential shape recorded from mammalian ventricular tissue has been reconstructed on the basis of two inward and two outward current systems for which (with the exception of activation kinetics for the fast inward current) experimental evidence exists (Beeler and Reuter, 1977; Trautwein and McDonald, 1978); that of the rhythmically active Purkinje fiber has been computed using nine distinguishable currents (McAllister et al., 1975). We have recently reviewed the relations between the nine conductances of the McAllister-Noble-Tsien model and the spontaneous oscillatory properties of the heart (DeHaan and DeFelice, 1978).

All of the above analyses of cardiac membrane currents have been performed on adult heart tissue. Until now, voltage clamp data defining current-voltage relationships in embryonic cardiac preparations have not been available. Evidence concerning the identity and kinetics of ionic currents in such preparations has been indirect, based upon action potential parameters and the sensitivity of electrical events to (adult) current inhibitors. For example, tetrodotoxin (TTX), which specifically blocks the fast-transient inward sodium current (I_{Na}) in nerve, skeletal muscle, and adult cardiac tissue (reviewed by Narahashi, 1974), has no effect on hearts from embryonic chicks, 2–4 d of age, even at concentrations up to 3×10^{-5} M. However, after 7 d of development, spontaneous activity can be inhibited by TTX concentrations as low as 3×10^{-8} M (Ishima, 1968; Shigenobu and Sperelakis, 1971; McDonald et al., 1972). On the other hand, the organic compounds, verapamil and D600, which suppress the slow inward current (I_{si}) in adult cardiac tissue (Kohlhardt et al., 1972; Kass and Tsien, 1975), can abolish action potentials in hearts from embryos up to 3 d of age, whereas in hearts 7 d or older, these drugs merely reduce the amplitude and duration of the plateau phase; they do not affect action potential generation at these later stages (Shigenobu et al., 1974; McDonald and Sachs, 1975).

In this paper we report on a voltage clamp analysis of a heart tissue model system consisting of a spheroidal aggregate of embryonic ventricular cells in culture (Sachs and DeHaan, 1973). We have shown previously that the cells within such an aggregate are tightly coupled electrically. The entire aggregate membrane appears to be virtually isopotential during the voltage changes produced by injecting small current pulses through an intracellular micropipette (Clay et al., 1978), although it deviates somewhat from uniformity during the fast rise time of an action potential (DeHaan and Fozzard, 1975). Junctional impedance between cells is $<10\%$ of transmembrane impedance and is independent of intercellular voltage gradients in the range of 10^{-5}–10^{-2} V, from DC to 160 Hz (DeFelice and DeHaan, 1977). In the present report, we test further the degree of spatial homogeneity in this preparation under voltage clamp conditions, when substantial currents are applied in fast-rising steps. With the aid of an exploring voltage electrode, we show that deviation from voltage homogeneity during a clamp step is comparable to that achieved in adult cardiac

preparations. We also demonstrate two kinetically and pharmacologically distinct components of inward current and a delayed outward current with properties similar to those observed in adult heart tissue. The advantages of spherical geometry and small size for voltage clamp analysis have also been exploited in a cultured preparation of neuroblastoma cells, 60–110 μm in diameter (Moolenaar and Spector, 1978).

METHODS

Tissue Culture

Culture techniques for the preparation of embryonic heart cell aggregates have been described in detail elsewhere (DeHaan, 1970; Sachs and DeHaan, 1973). Briefly, fertilized eggs from White Leghorn chickens were incubated for 7 d at 37°C. Cells were dissociated from fragments of ventricles by a multiple-cycle trypsinization procedure (DeHaan, 1967), and allowed to aggregate in medium 818A (DeHaan, 1970) during a 72-h period on a gyratory shaker (60–67 rpm, 1.25-in stroke).

Aggregates attached to the bottom of a 35-mm tissue culture dish (Falcon Plastics, Oxnard, Calif.) were maintained at 35–37°C on the heated stage of a dissecting microscope. A mixture of 5% CO_2, 10% O_2, and 85% N_2 was passed through a toroidal gassing ring surrounding the dish, and maintained the pH at 7.4. All experiments were performed in 4 ml of a 3:1 mixture of medium 818A (DeHaan, 1970) and medium 21212 (Nathan et al., 1976) with the following final composition (millimolar per liter): NaCl 124; KCl 4.6; $CaCl_2$ 1.4; $MgCl_2$ 0.4; $MgSO_4$ 0.6; NaH_2PO_4 0.7; Na_2HPO_4 0.7; $NaHCO_3$ 17; and dextrose 5.5.

Electrophysiology

Glass micropipettes were prepared by the glass fiber technique (Tasaki et al., 1968) and filled with 3 M KCl. Electrodes with resistances between 10 and 25 MΩ were selected for voltage clamping. Intracellular electrodes were coupled through Ag-AgCl holders to capacitance-compensated, unity-gain electrometer amplifiers, A_2 and A_3 (Fig. 1 F) (Instrumentation Laboratory, Inc., Lexington, Mass., Picometric, model 181). Intracellular potentials were recorded with respect to the bathing medium which was coupled to a virtual ground through two agar-KCl bridges, connected in parallel to reduce series resistance.

The double-microelectrode voltage clamp technique (Deck et al., 1964; Hecht et al., 1964) was employed with standard circuitry (Cole and Moore, 1960) as illustrated diagrammatically in Fig. 1 F. Potentials up to 140 V were provided by a high-output variable gain operational amplifier A_1 (Analog Devices, Inc., Norwood, Mass., model 171K) in the inverting configuration, and currents were recorded as the voltage drop across the feedback resistor (100 kΩ) of the virtual-ground operational amplifier, A_4 (Analog Devices, Inc., model 48K). Command potentials, consisting of steps provided by a digital pulse generator (Frederick Haer & Co., Ann Arbor, Mich., Pulsar, model 4) and the holding potential, were added to the membrane potential at the summing junction of the control amplifier A_1. Its gain was sometimes reduced to avoid oscillations in current that occasionally followed the on- or off-transients of a large voltage step. These oscillations may have been induced partly by capacitive coupling between the current-passing and voltage-recording electrodes since a grounded shield was not used. Following a command step (V_c), the potential recorded by electrode V_1 (in the feedback loop) usually reached its new steady value in about 0.4 ms. This delay was not prolonged by a slight reduction in the gain of amplifier A_1.

Potentials recorded from two or three intracellular microelectrodes and membrane currents were amplified by low-noise operational amplifiers (Analog Devices, Inc., model 504M) and recorded on FM tape (Sangamo Weston, Inc., Springfield, Ill., Sabre, model

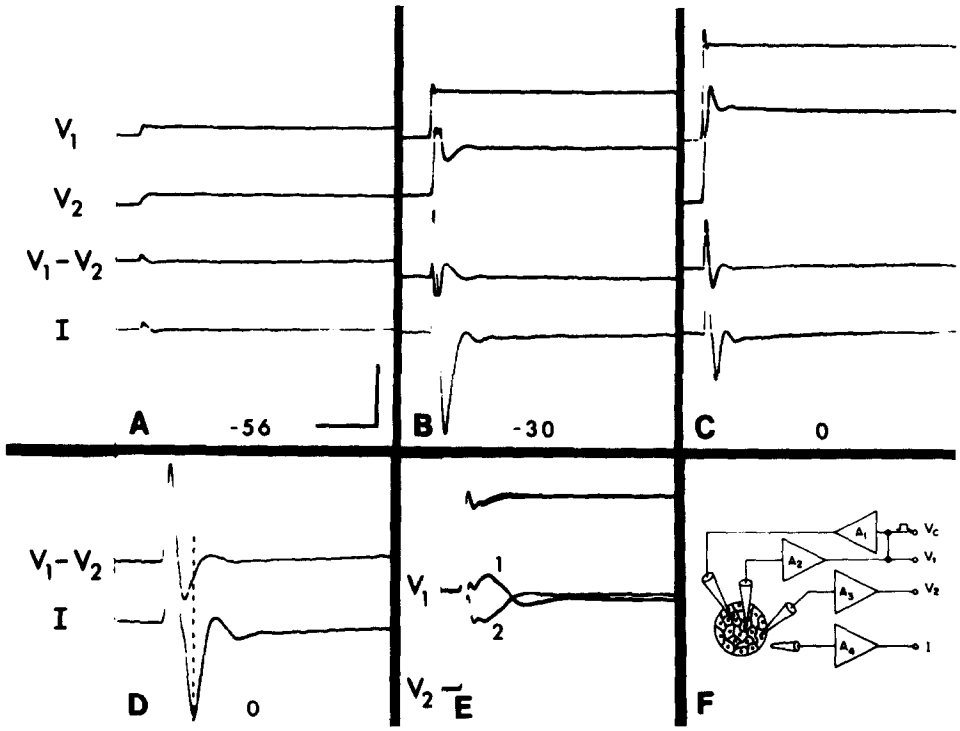

FIGURE 1. Three-microelectrode voltage clamp tests of spatial homogeneity in aggregates. As illustrated in panel F, V_1 is the recorded potential used in the feedback loop; V_2 is an exploring intracellular electrode independent of the feedback loop; $V_1 - V_2$ is a measure of the deviation from isopotentiality; I is total membrane current. V_2 was placed in line with V_1 and the current source as illustrated in (F) for (A) and (C), i.e., 30–50 μm from V_1 and about 100 μm from the current source; V_2 was placed in line between V_1 and the current source i.e., 30–50 μm from each electrode in (B). Panel D is a faster sweep of (C). In (E) trace 1 was obtained with V_2 close to the current source, and trace 2 with V_2 far from the current source. Holding currents (currents required to maintain the membrane at the holding potential) were −5 nA (A) and −40 nA (B) and (C), at −62 mV and −60 mV, respectively. Aggregate impaled in panel B was exposed to 1.67×10^{-7} g/ml cytochalasin B. The records in panels A–E were obtained from four different aggregates, all having diameters of 144 ± 7 μm. Vertical scale: V_1 and V_2, 40 mV; $V_1 - V_2$, 40 mV in panels A, B, and C; 20 mV in panel D; I, 1 μA in A, B, and C; 0.5 μA in D. Horizontal scale: 10 ms in A, B, and C; 4 ms in D and E.

2; or Hewlett-Packard Co., Palo Alto, Calif., model 3960) at a speed of 3¾ in/s (bandwidth, DC to 1.25 kHz). At this speed, the waveform of the fast inward transient was not distorted significantly by the recorder. Control recordings of voltage ramps with

slopes of 0.9-1.5 V/ms were reduced in amplitude by <10%. These were comparable with the fastest rates we recorded (e.g., Fig. 1 D). On the other hand, the much faster rise times of square-wave voltage steps and capacitive transients were presumably distorted by the tape recorder, and were recorded with damped oscillations after their onsets (see V_1, Fig. 1 C) and offsets (Fig. 9).

Data Analysis

All measurements of membrane current magnitudes and kinetics were made directly from the oscilloscope CRT during replay of the tapes. Because of variation in the absolute magnitude of currents recorded among different aggregates and for different impalements within the same aggregate, we were unable to determine a current-voltage relationship for leakage currents, (Such a correction would have required recording leakage after blocking the dynamic currents with TTX, D600, Cs, etc., replacing these drugs with the standard medium, and then recording the time-dependent currents, all from the same aggregate and ideally during the same impalement.) Rather, both inward and outward currents were adjusted for leakage only at the "holding potential"; i.e., they were determined with respect to the "holding current" (current required to maintain the membrane at the holding potential) preceding each voltage step. Thus, since leakage currents were not corrected for (and likely increased) during clamp steps, our inward, and especially our outward currents are probably somewhat overestimated. In preparing the current-voltage relationship shown (Fig. 6), dynamic currents preceded by large holding currents were not included.

Time constants for the decay of inward currents were obtained by measuring changes in total current with time from oscilloscope traces and using these values in an asymptotic regression analysis of the function $A + Be^{-t/\tau}$. The relatively long duration of the capacitive transient precluded an analysis of the fast transient inward current's activation kinetics.

Aggregates used for this study varied from 120 to 180 μm in diameter. Net currents were referred to total cell surface area for calculation of specific currents. Aggregates were viewed at a magnification of × 62, and their major and minor axes were measured with an ocular reticle whose smallest division represented 36 μm. Measurements could be made accurately to about 0.2 divisions (7 μm). Total aggregate volumes (V_A) were obtained using the equation for a prolate spheroid, $V_A = 4/3\ \pi ab^2$, where a and b represent the major and minor hemi-axes. The number of cells per aggregate (N_A) was calculated by two different methods. Isolated ventricle cells in suspension were spherical in shape until they adhered to the surface of the substratum or other cells. The mean cell diameter measured from 1,545 cells before aggregation was 10.8 ± 0.9 μm,[1] yielding a mean cell volume (V_C) of 660 μm^3. As confirmed in electron micrographs,[2] this volume does not change significantly when these cells are closely associated within spheroidal aggregates. In addition, we have shown that total aggregate volume consists of 80% cells and 20% extracellular space (McDonald and DeHaan, 1973; Elsas et al., 1975). Thus, the number of cells per aggregate could be calculated by $N_A = 0.8\ V_A/V_C$. N_A was also estimated by measuring aggregate DNA content using an observed value of 2.8 pg DNA per cell, measured in single ventricular cell suspensions and chicken erythrocytes (Santora et al., 1978). Total DNA per aggregate was determined from pooled groups of counted, sized aggregates by the method of Giles and Meyers (1965) or by a modified ethidium bromide spectrofluorometric method.[3] The mean cell volume calculated from

[1] Atherton, B., and R. L. DeHaan. Unpublished data.
[2] Baste, C. A., and R.L. DeHaan. Unpublished data.
[3] Kellar, K., and J. M. Kinkade. Unpublished data.

the aggregate DNA assays was 651 μm^3. Thus, estimates of N_A derived from the two methods agreed within ± 1%. Total cell surface area per aggregate was calculated as the product of the number of cells per aggregate and the mean surface area per cell (366 μm^2). The total membrane area of a spheroidal aggregate 150 μm in diameter is 7.8×10^{-3} cm^2. Aggregates used in voltage clamp experiments ranged in size from 119 × 126 μm (4.0×10^{-3} cm^2) to 173 × 180 μm (11.9×10^{-3} cm^2). In calculating the total active membrane area, no correction was made for non-cardiac cells, which probably represented <20% of the aggregate population (Sachs and DeHaan, 1973).

Drugs

Tetrodotoxin (Calbiochem, San Diego, Calif.) and compound D600-hydrochloride (Knoll Pharmaceutical Co., Whippany, N. J.) were dissolved in distilled water to make stock solutions of 1.0 mg/ml and 0.1 mg/ml, respectively. For some experiments, aggregates were incubated overnight in 1.67×10^{-7} g/ml cytochalasin B (Calbiochem) to disrupt myofibrils and prevent contraction (Sachs et al., 1974). The cytochalasin B was dissolved in dimethylsulfoxide to make a stock solution of 0.1 mg/ml. All drug concentrations are expressed in units of grams per milliliter in order to compare directly with values used by other investigators.

Voltage Control

The potential difference ($V_1 - V_2$) between different cells in an aggregate may be taken as a direct measure of intracellular homogeneity (excluding external series resistance, discussed below) (New and Trautwein, 1972; Reuter and Scholz, 1977). With an exploring intracellular electrode (V_2) in the configuration shown in Fig. 1 F, the degree of voltage homogeneity during voltage clamp steps was generally dependent upon the magnitude of the current passed into the aggregate. For small voltage steps, for example, to −56 mV (Fig. 1 A) where I_{Na} was only partially activated (−43 nA), $V_1 - V_2$ was never >1 mV. For larger depolarizing steps (−30 mV, Fig. 1 B), where I_{Na} was almost maximal (−1.57 μA), $V_1 - V_2$ was ~8 mV at the time of apparent peak inward current. For a still larger voltage step to 0 mV (Fig. 1 C, D), I_{Na} was reduced (−0.72 μA), and $V_1 - V_2$ was only 4 mV during peak inward current. Although these measurements were made on several different aggregates, our ability to select preparations of uniform size resulted in data of an acceptable degree of reproducibility. Voltage homogenity was usually better with steps that produced little current (Table I), and better during slow inward transients than during fast. With large clamp steps, reasonable control was reached within 3–5 ms. Deviation from homogeneity was greatest during the capacitive transient; uniformity always improved during the decay of I_{Na} (Fig. 1 D). Mean deviation from isopotentiality at the time of maximal activation of I_{Na} was 6.4 ± 0.7 mV (mean ± SE), or 12% in 13 experiments. After the fast inward current had inactivated, $V_1 - V_2$ was usually <2 mV.

Fig. 1 E illustrates the effect of electrode position on the potential recorded by the test electrode (V_2) during a 60-mV depolarizing clamp step. This experiment was performed (without having to move the electrodes physically) by reversing the V_1 and V_2 electrode inputs to their respective amplifiers, A_2 and A_3, just before the second of two consecutive steps to 0 mV. During the first step (trace 1), the test electrode was located between the current source and V_1; the test electrode was then switched to amplifier A_2, and the most distant electrode to A_3 (effectively reversing the positions of V_1 and V_2). When V_2 was far (100 μm) from the current source (trace 2), the development of potential was delayed; when close to the current source (30–50 μm), the potential recorded by V_2 overshot the command potential by almost 10 mV (trace 1). The rapid initial transient (<0.5 ms) in each trace (Fig. 1 E), due mainly to charging of the membrane capacitance, may have also been influenced by capacitive coupling between the current source and voltage

electrode. Although the potential seen at V_1 did not vary with position since it was controlled directly by the clamp, the shift in V_2 indicates that for a 60-mV step, a gradient of current lasting ~3 ms spread outward from the current source. With greater separations between V_1 and the current source (>100 μm), slight deviations of V_1 from the command potential might be expected.

Stability of Membrane Currents

Damped oscillations, possibly due to capacitive coupling between the current and voltage electrodes, were sometimes observed in relation to the capacitive surge following the

TABLE I

MEASUREMENT OF VOLTAGE HOMOGENEITY WITH AN EXPLORING ELECTRODE

V_1	I_h	I_{Na}	I_{si}	MDP(I)	MDP(V_1)	MDP(V_2)	V_2	V_1–V_2
mV	*nA*	*nA*	*nA*	*mV*	*mV*	*mV*	position	*mV*
−60*	−5	–	–	−73	−76	−79	F	<1
−58*	−5	−40	0	−73	−76	−79	F	<1
−56*	−5	−43	0	−73	−76	−79	F	−1
−54*	−10	−56	0	−73	−76	−79	F	−1
−31‡	−200	2,200	−176	−77	−77	−75	F	−4
−30‡	−40	1,570	−150	−72	−76	−70	C	+8
0	−40	−720	−110	−62	−71	−71	F	−4
0	−75	−325	−50	−58	−60	−58	F	−5
0‡	+10	−822	−135	−77	−77	−75	F	−6
0‡	−25	−525	−113	−69	−66	−68	F	−12
0	−5	−850	−90	−68	−67	−64	F	−9
0	0	−950	−60	−60	−60	−60	C	−4
0	−10	−1,330	−110	−70	−70	c−76	C	+4
0	−88	−675	−100	−62	−74	−75	S	+9
0	−240	−1,110	−100	−67	−67	−70	S	+4
0	−150	−940	−90	−60	−65	−65	S	+7
0	−25	−663	−150	−73	−73	−73	S	−7

V_1, value of step potential recorded by V_1 electrode. I_h, holding current required to maintain membrane potential at −60 mV. I_{Na}, peak fast inward current with respect to the holding current. I_{si}, peak slow inward current with respect to the holding current. MDP, maximum diastolic potential during spontaneous activity recorded just before voltage clamp by current source (I) and V_1 and V_2 electrodes. V_2 position, position of the exploring electrode (V_2) with respect to the current source (I) and voltage electrode (V_1). F (far) indicates that V_1 was placed in line between I and V_2, with a 30–50 μm spacing between each electrode. C (close) indicates that position of V_1 and V_2 is reversed with respect to I. S (symmetric) indicates that I, V_1, and V_2 formed the vertices of an equilateral triangle, approximately 100 μm on a side. V_1–V_2, deviation from homogeneity determined at the time of peak fast inward current.

* Holding potential, −62 mV.

‡ Aggregates incubated overnight in 1.67×10^{-7} g/ml cytochalasin B, to abolish mechanical contraction (Sachs et al., 1974).

onset (Figs. 1 D and 8 B) or offset (Fig. 9 B) of large voltage steps. The amplitude of these oscillations declined with repeated steps or with increased external series resistance, and could also be reduced by decreasing the gain of the control amplifier without significantly affecting voltage control.

The magnitude and rates of decay of both the capacitive transient and the fast inward current (at potentials positive to −20 mV) sometimes declined a small amount during repeated clamp steps to the same potential. In seven experiments, I_{Na} decreased 13.4 ±

4.9% (mean ± SE) between the first and fourth repeated clamp step. These changes, together with a concomitant rise in holding current, suggested that aggregate series resistance probably increased during repeated passage of significant ionic current (see Discussion). Whenever such distortions were observed, only the first step in a sequence of potentials was used in further analyses.

RESULTS

Series Resistance

Because it is not possible to ground the volume immediately adjacent to the entire aggregate membrane, current flowing across the membrane must pass through an "access resistance" in series with the membrane itself. This includes an external component—mainly the intercellular clefts, the bath volume, and the agar bridges—and the intracellular resistance of the cytoplasm and nexal junctions. To calculate this series resistance (R_s), we have neglected "cable" properties and leakage pathways and have assumed an equivalent circuit with lumped resistance (R_m) and capacitance (C_m) in parallel to represent the cell membrane. A single resistor in series with the membrane is used to represent both intracellular and extracellular series resistance. At the onset of a voltage step, when ideally $t \rightarrow 0$, all current flows as charge displacement across the membrane capacitance; thus,

$$R_s = \frac{\Delta V_c}{I_c}, \tag{1}$$

where I_c is the peak capacitive current and V_c is the command potential. Slightly different calculations of series resistance in multicellular preparations have been made by Attwell and Cohen (1977). From a series of voltage steps in the range of 5–25 mV, where decay of the capacitive current could be fit with a single exponential, the mean values of R_s (± SE) calculated from Eq. 1 was 22.7 ± 2.2 kΩ. Since two agar-KCl bridges, each with a resistance of about 10 kΩ, were connected in parallel in these experiments, the series resistance presented by the aggregate alone (i.e., intercellular clefts, cytoplasm, and nexal junctions) was about 17 kΩ. This value might be somewhat in error due to the influence of possible capacitive coupling between the current and voltage electrodes (which would tend to increase transiently ΔV_c and I_c), and because of the slow tape recorder response (which would tend to reduce I_c and therefore increase R_s). The extent to which these errors would cancel is not clear.

Current Magnitudes and Kinetics

We were not able to separate clearly the capacitive transient, which generally lasted ~ 1.5 ms, from the onset of I_{Na} (for example, Fig. 1 D). Thus, an accurate analysis of the activation kinetics of I_{Na} was not possible, and our values for peak I_{Na} may be somewhat underestimated.

In medium containing 4.6 mM KCl, aggregates beat spontaneously with a mean maximum diastolic potential of −70 mV (Table I) before application of the voltage clamp; nonetheless, a holding potential of −60 mV seemed to

minimize holding currents. From this potential, peak I_{Na} during a step to −20 mV was about seven times greater than the peak slow inward current (I_{si}) at 0 mV. At −30 mV (Fig. 2 A) where I_{Na} approached its maximum value, I_{si} was small; while at 0 mV (Fig. 2 B), I_{si} (arrow) was maximal and I_{Na} was reduced.

The fast and slow components of inward current reached their respective peaks 2.6 ± 0.3 ms and 6.8 ± 0.3 ms (mean ± SE, n = 35) after the onset of voltage steps, and these times underwent no dramatic changes between −50 and + 40 mV. The decay of each component could be fit by a single exponential (Fig. 3), and time constants for I_{si} were 10–30 times greater than those calculated for I_{Na}. The decay kinetics of I_{si} were influenced strongly by membrane potential (Fig. 4) and were most rapid at −20 mV. In these experiments, net current was measured at 5-ms intervals between 10 and 40 ms after onset of a step, and no correction was made for the influence of outward currents, which would have tended to shorten time constants at more positive potentials. Most of these results were obtained in the presence of TTX (●) to remove the influence of

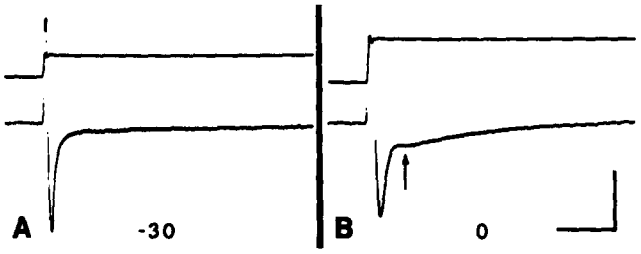

FIGURE 2. Fast and slow (arrow) components of inward current (downward) during voltage clamp steps to −30 and 0 mV. Holding potential, −60 mV; holding current, −2 nA (A) and 0 nA (B); aggregate diameters, 135 μm (A) and 144 μm (B). Horizontal scale: 10 ms. Vertical scale: 80 mV, 0.5 μA.

I_{Na}, but the few values obtained in normal media (○) suggested that neither I_{Na} nor TTX itself had a large effect on the decay kinetics of I_{si}.

Current-Voltage Relationships

Fig. 5 illustrates a series of 400-ms steps to potentials between −50 and −10 mV. At −50 mV fast inward current was only partially activated. At more positive potentials, I_{Na} became maximally activated (−30 mV), and the slow component increased (Fig. 5 E). Outward current (measured from the holding current preceding each step) was small for potentials negative to −20 mV, but began to increase significantly at more positive potentials. The slow development of a large outward current at −10 mV which was not present at −30 mV indicates the appearance of delayed rectification. The increasing magnitude of inward-going tails at the end of steps at −30 to −10 mV may be attributed to a steady-state component of I_{si} (i.e., $I_{si} = f_\infty d_\infty \bar{I}_{si}$), whose activation increases (inactivation decreases) with more positive potentials (Bassingthwaighte and Reuter, 1972), or may reflect an increased leakage current as a result of myofibrillar contraction during the step.

Fig. 6 illustrates the voltage dependence of inward and outward currents over the range from −82 to +40 mV obtained from 19 aggregates. Peak I_{Na} was maximal at about −20 mV (−185 μA/cm^2). In TTX, slow inward current (at 10 ms) was maximal near 0 mV and reached a mean value of −20 μA/cm^2. The threshold for activating I_{si} was 20–30 mV positive to that for I_{Na}. The magnitude of I_{si} was not corrected for outward-going current and therefore may be underestimated at positive potentials. Thus, the true reversal potential for I_{si} may be more positive than the value shown. The reversal potential for I_{Na} was calculated to be +38.5 mV on the basis of the intracellular concentration of Na^+, measured in 7-d chick heart cell aggregates (McDonald and DeHaan, 1973).

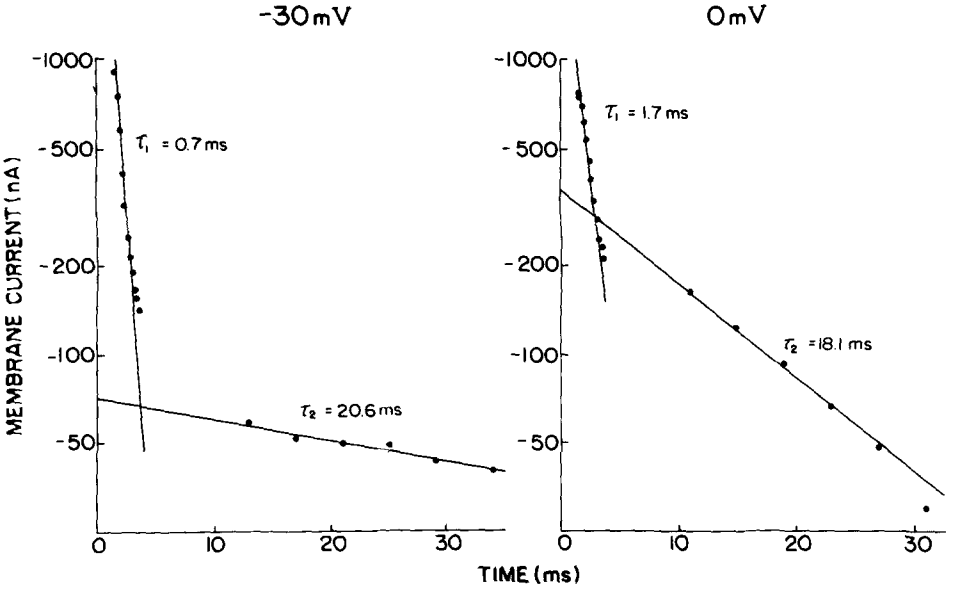

FIGURE 3. Logarithmic plots of the exponential decay of fast and slow components of inward current in Fig. 2. Experimental values of total current (●) were obtained at 0.4-ms (τ_1) or 4-ms (τ_2) intervals, beginning just after each peak and were fit by eye (solid lines).

Pharmacological Effects

Fig. 7 illustrates the effects of TTX and D600 on action potentials recorded from 7-d heart cell aggregates. TTX in concentrations as low as 10^{-8} g/ml blocked spontaneous activity in 7-d aggregates. However, when action potentials were stimulated electrically in the presence of TTX, their maximum upstroke velocities were reduced from > 120 V/s (Fig. 7 B, trace 1) to < 20 V/s (trace 2). Note that the plateau phase of the action potential was not affected significantly (Fig. 7 A, trace 2). D600, at a concentration of 5×10^{-7} g/ml, reduced the amplitude and duration of the plateau dramatically (Fig. 7 C, trace 2) without affecting spontaneous activity, the overshoot potential or upstroke velocity (Fig. 7 D, trace 2). However, the combination of TTX and D600 (not illustrated) blocked generation of the action potential, even with intense electrical stimulation. The effects of TTX could be reversed by changing the bathing medium, but this was not the case with

D600. A complete reversal of its action took place only gradually over a period of 1 h or more.

The effects of TTX and D600 on membrane currents were consistent with their influence on the action potential. Fast and slow sweeps of control currents generated

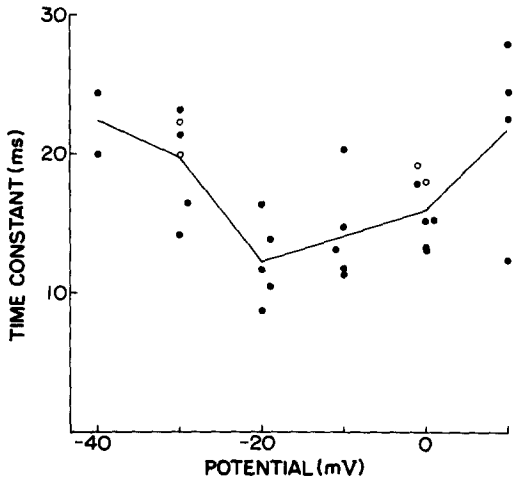

FIGURE 4. Voltage dependence of slow inward current decay kinetics. Time constants were calculated from measured values of total current in the presence (●) or absence (○) of TTX (1.25×10^{-6} g/ml) which were used in a regression analysis of the function $A + Be^{-t/\tau}$. The solid line is drawn through the mean value at each potential.

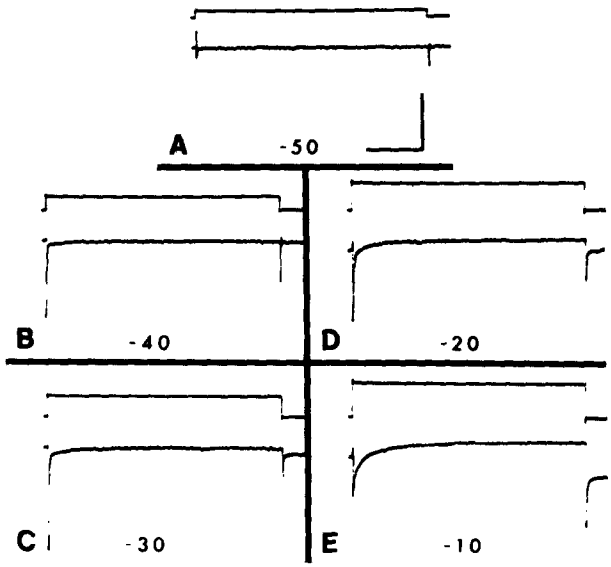

FIGURE 5. Membrane currents during consecutive 400-ms steps in a 135-μm diameter aggregate. Holding potential, −60 mV; holding currents, 0 nA (A), −5 nA (B), −2 nA (C), −70 nA (D) and −75 nA (E). Horizontal scale: 100 ms. Vertical scale: 80 mV, 0.5 μA.

during a 400-ms step from −60 mV to 0 mV are illustrated in Figs. 8 A and 9 A. D600 (5×10^{-7} g/ml) blocked the slow inward current (Fig. 8 B), reduced outward current activation and increased net outward, time-independent current (Fig. 9 B). The upward deflection which follows the fast inward transient (Fig. 8 B) is most likely part of the damped oscillation generated by capacitive coupling (see Methods; see also the oscillation following the offset of the step, Fig. 9 B). TTX (1.25×10^{-6} g/ml) blocked the fast component of inward current but did not affect the slow component or outward-going

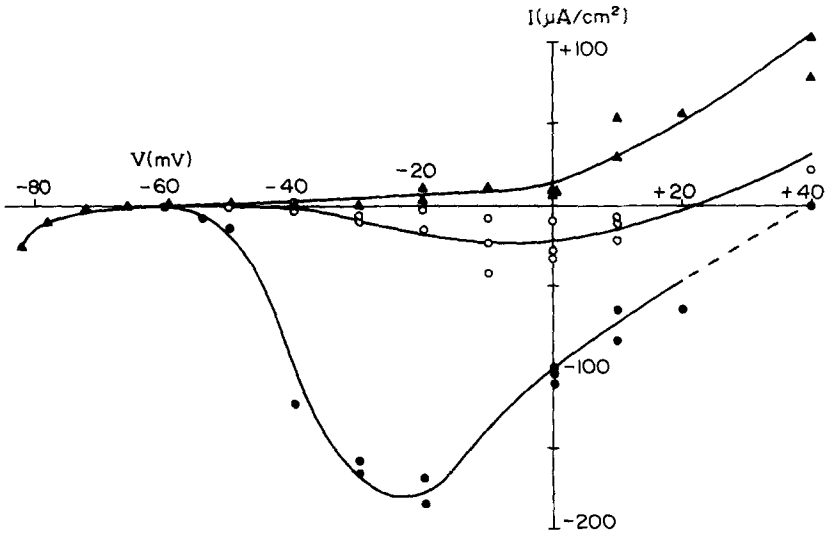

FIGURE 6. Current-voltage relationships of aggregates in normal media for peak fast inward current (●), net outward current at 400 ms (▲), and for net inward current in TTX (1.25×10^{-6} g/ml) measured at 10 ms (○). Slow inward current was never >30% greater at its peak than at 10 ms. All currents were measured with respect to the holding current preceding the voltage step and were not corrected otherwise for leakage currents or for outward-going currents. Of the 37 measurements illustrated in this curve, 24 were preceded by holding currents ≤10 nA, the remainder were <50 nA, and the points were derived from a total of 19 aggregates. Clamp currents were converted to current densities by referring to total cell surface area of each aggregate. Smooth curves were fitted by eye through the mean value at each potential. Holding potential was −60 mV in all cases. The reversal potential for peak fast inward current (+40 mV, ●) was determined as the potential at which the current changed directions from inward- to outward-going. The dashed line represents a smooth extension of the curve through the reversal potential.

current (Figs. 8 C and 9 C). In Figs. 8 D and 9 D, TTX (1.25×10^{-6} g/ml) was added to an aggregate already affected by D600 (5×10^{-7} g/ml). The combination of the two drugs blocked both components of inward current leaving only time-independent outward current (Fig. 9 D). Prolongation of the capacitive transient in TTX (Fig. 8 C) and in D600 + TTX (Fig. 8 D) may have resulted from increased membrane input resistance in the presence of these drugs, or may represent its true waveform, which had been shortened in the control experiment (Fig. 8 A) by the rapid onset of the fast inward current.

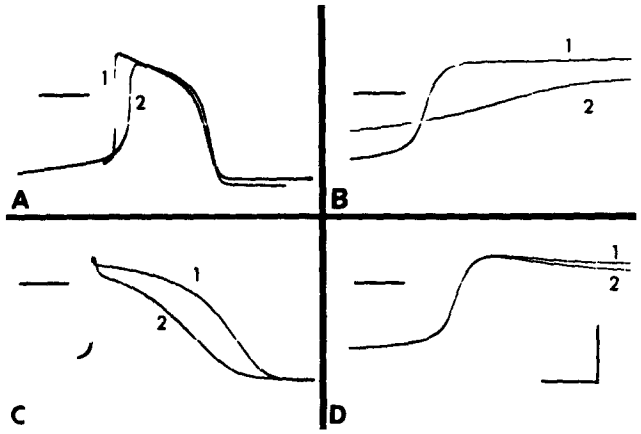

FIGURE 7. Action potentials recorded during continuous impalement of two untreated aggregates (traces 1) and after exposure (traces 2) to TTX (10^{-5} g/ml) (A) and (B), and to D600 (5×10^{-7} g/ml) (C) and (D). Maximum upstroke velocities of the controls were 153 V/s (B, trace1) and 137 V/s (D, trace 1). TTX slowed the upstroke velocity to 12 V/s (B, trace 2) 2 min after its addition. Note that the plateau was not affected significantly (A). D600 reduced the amplitude and duration of the plateau (C, trace 2) but did not affect the upstroke velocity (D, trace 2). Horizontal scale: 100 ms, (A); 40 ms, (C); 1 ms, (B) and (D). Vertical scale: 50 mV. Horizontal lines represent 0 mV.

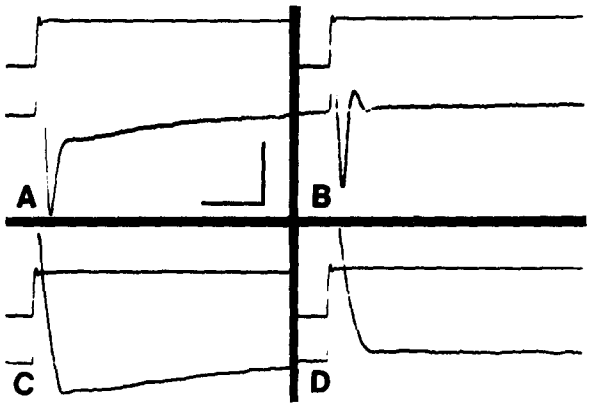

FIGURE 8. Effects of drugs on membrane currents during voltage clamp steps to 0 mV. A, Control. B, D600 (5×10^{-7} g/ml). C, TTX (1.25×10^{-6} g/ml). D, D600 (5×10^{-7} g/ml) and TTX (1.25×10^{-6} g/ml). Holding potential, −60 mV; holding currents, 0 nA (A), −10 nA (B), −4 nA (C), and −30 nA (D). (A) and (C) were recorded from one aggregate, diameter 140 μm; (B) and (D) were from a different aggregate, diameter 151 μm. Horizontal scale: 10 ms. Vertical scale: 80 mV, 0.5 μA.

DISCUSSION

Voltage Control

The most severe limitation on the voltage clamp technique as applied to cardiac tissue has been lack of voltage control, i.e., spatial inhomogeneity (Johnson and Lieberman, 1971; Fozzard and Beeler, 1975). With an exploring intracellular electrode independent of the clamp feedback circuit, several investigators have demonstrated uncontrolled voltage changes in ostensibly "clamped" regions of the tissue, even when the command voltage electrode exhibited virtually perfect control (Beeler and Reuter, 1970*a*; New and Trautwein, 1972; McGuigan, 1974; Tarr and Tank, 1974; DeHemptinne, 1976). Nonetheless, technical improvements have been made in clamp circuitry and in the preparation itself to minimize deviations from voltage homogeneity and permit meaningful analyses

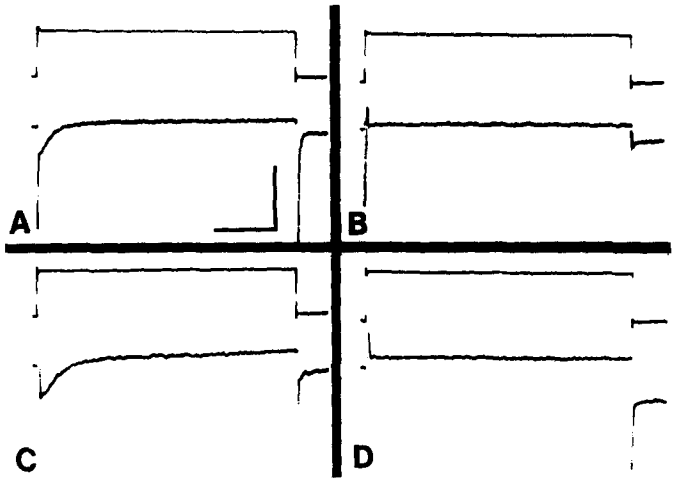

FIGURE 9. Slow sweeps of steps in Fig. 8. Horizontal scale: 100 ms. Vertical scale: 80 mV, 0.5 μA. Pulse duration, 400 ms. Note the absence of outward current activation (B and D) and the slight increase in time-independent outward current in D.

of the I_i (V) relations (New and Trautwein, 1972; DeHemptinne, 1976; Goldman and Morad, 1977).

The requirements for an optimal cardiac preparation appear to be a low intercellular resistance, a minimal ratio of length to diameter and an overall small size to minimize the total membrane to be controlled. Although the embryonic heart cell aggregates analyzed in the present study meet the criterion of overall small size (120–180 μm in diameter), the small diameter of individual myocytes, 10–12 μm (and therefore the large number of cells per aggregate) dictates a significant total membrane surface area and series resistance. Our results with an exploring voltage electrode have shown that such aggregates deviate from isopotentiality by 6.4 ± 0.7 mV (mean ± SE), or 12%, during the first 3-5 ms of clamp steps, when the fast transient inward current was maximally activated, and by < 2 mV (~ 3%) thereafter. These values are comparable with those measured in adult cardiac tissue during peak I_{Na} (Fig. 6, New and

Trautwein, 1972; Fig. 7, DeHemptinne, 1976) and during I_{si} (Fig. 4, Reuter and Scholz, 1977). Haas et al., (1971) reported (but did not illustrate) deviations of only 2 mV during the flow of fast inward current. However, the "fast" inward currents they recorded were much slower (20-ms duration) than in other investigations (see Fig. 1, Haas et al., 1971). We have also seen maximal deviations of 2–3 mV during some clamp steps, but only when I_{Na} was slowed greatly would there be increased series resistance.

Potential gradients of several mV during the first 3-5 ms of a voltage clamp step would result in a spatial distribution of magnitudes and kinetics of recorded currents. For I_{Na} this spread of magnitudes would be greatest at the point of maximal negative slope conductance (about −40 mV, Fig. 6). For example, a 10-mV spread about −40 mV would yield a range of currents from −50 to −145 $\mu A/cm^2$. The total inward current recorded in the bath for a step to −40 mV would be a weighted sum of values between these two extremes and would also include values generated (at other potentials) in other regions of the aggregate. The weighting function would be the spatial distribution of current emanating from a point source within the aggregate. It is probably safe to assume that the cells that would deviate most from the command potential would lie between the current source and the potential-sensing electrode (V_1). Because of the decay of potential radially from the point source, these cells would be more positive than V_1 during a depolarizing clamp step. This is exactly what was observed with the exploring electrode (trace 1, Fig. 1 E). Thus, inward-going currents are likely to be overestimated in the negative-slope regions of our current-voltage relationships (Fig. 6) and underestimated in the positive-slope regions. Such a shift of these curves toward more negative values is also expected as a result of the direct effects of series resistance. Delayed outward currents would not be greatly affected inasmuch as spatial homogeneity was better than 97% after the first 5 ms of a voltage step.

Series Resistance

The fact that aggregates contain a large extracellular volume suggests that the intercellular cleft spaces may be in good electrical contact with the external bathing medium. The value of 20% extracellular space is similar to that for adult ventricle but larger than for cardiac Purkinje fiber preparations (Hellam and Studt, 1974). Moreover, embryonic heart cells lack a transverse tubular system (Hirakow and Gotoh, 1975), and the aggregates are not surrounded by an appreciable endothelial layer that adds a substantial component of access resistance to adult preparations (Attwell and Cohen, 1977).

Our mean value for the aggregate series resistance (17 kΩ) is comparable to that reported by DeHemptinne (1976) for frog atrial trabeculae in a sucrose gap preparation. Other measurements on the same preparation have led to widely-varying values, from 2 kΩ (Goldman and Morad, 1977) to 99 kΩ (Connor et al., 1975) depending on the fiber diameter, node width, and other variables. In dog, cat, and cow ventricular trabeculae, values for series resistance as low as 0.3-0.6 kΩ have been reported (Beeler and Reuter, 1970*a*; New and Trautwein, 1972; Reuter and Scholz, 1977).

Because the series resistance prevents measurement of potentials directly

across heart cell membranes, any demonstration of spatial homogeneity, including our own, must be viewed with caution. For example, a negligible difference in the intracellular potentials recorded from two different cells (V_1 and V_2) within an aggregate might also be interpreted in terms of four different potentials which tend to cancel

$$V_1 = V_{m_1} + V_{s_1} = V_{m_2} + V_{s_2} = V_2, \tag{2}$$

where V_m is the voltage drop across the membrane and V_s is the drop across the series resistance. The actual membrane potentials would be equal only when R_s at the two points or measurement were equal, or negligibly small with respect to membrane resistance. The latter condition was probably very nearly approximated in our experiments at potentials near rest and in steady states near the plateau range (from −20 to +20 mV). At both voltage levels, R_m is high (Goldman and Morad, 1977; Noma and Irisawa, 1976; DeHaan and DeFelice, 1978). Even in the active state, since both electrodes usually penetrated cells deep within the aggregate and therefore "saw" approximately the same intercellular cleft resistance, V_{m_1} would equal V_{m_2} if V_1 were equal to V_2.

In the steady state (as $t \rightarrow \infty$), the current generated by a small voltage step can be expressed as

$$I_\infty = \frac{V_c}{R_m + R_s}. \tag{3}$$

The voltage drop across the membrane is

$$V_m = I_\infty R_m. \tag{4}$$

Substituting

$$V_m = V_c \frac{R_m}{R_m + R_s}. \tag{5}$$

Thus, the true membrane potential deviates from the command potential by the ratio of membrane resistance to total input resistance. When the membrane potential is near the resting level, $R_m >> R_s$, and V_m is nearly equal to V_c. From the slope of the current-voltage relation for outward current at −60 mV (Fig. 6), we estimate the specific input resistance at rest to be about 15 kΩ · cm². The clamp steps at that potential could be made with very small holding currents (11.2 ± 6.6 nA) which resulted in negligible leakage errors. This result agrees well with those from current pulse experiments in which the access resistance was referred to total cell surface area (DeHaan and Fozzard, 1975). In more recent experiments (Clay et al., 1978), currents of 0.1-1.0 nA were used to shift the membrane potential only 1-2 mV from known rest potentials; aggregate specific input resistance was measured at potentials between −66 and −70 mV to be 18 ± 2.5 kΩ · cm². Thus, near rest and for low frequency (i.e., steady state) conditions (Eq. 3), input resistance for a total cell surface area of 7.8×10^{-3}cm²) can be approximated by $(R_m + R_s) = 2\text{-}3 \times 10^6$ Ω. Since R_s (including bridges) was 2.3×10^4 Ω (see Results), $R_m/(R_m + R_s) = 0.99$, and V_m differed from V_c by only 1%.

In the active state, voltage-dependent sodium channels open and membrane resistance collapses. Using the positive slope of the I_{Na} current-voltage relation at 0 mV (Fig. 6), we calculate a total apparent "controlled" resistance ($R_m + R_s$) of ~ 50 kΩ. In this case, $R_m/(R_m + R_s) = 0.54$. That is, membrane potential calculated from Eq. 5 is only 54% of clamp potential during peak I_{Na}. Similar large "error factors" during the fast transient due to series resistance have been acknowledged by DeHemptinne (1976).

Because the voltage drop across R_s is negative during the flow of inward current, an equal and opposite change is required across R_m to maintain the recorded potential (V_1) constant (Ramón, et al., 1975). This implies that relatively small depolarizing command steps (V_c) are seen by the membrane as much larger ones, resulting in a significant magnitude of inward current. For example, given an error factor of 54%, a step from −60 mV to −20 mV would result in a voltage drop of −18.4 mV across R_s and an excess of +18.4 mV across R_m. Thus, series resistance tends to increase the steepness of the negative resistance branch and shift the peak of our fast inward current-voltage relationship to the left, perhaps as much as 20 mV. Similar shifts have been predicted in computer simulations of multicellular preparations in voltage clamp (Ramón et al., 1975). Ideally, the reversal potential of I_{Na} would not be affected since zero current requires no voltage drop across R_s; however, the presence of I_{si} and outward currents at that potential negate this argument. The magnitude of the error will depend upon the magnitude of membrane conductance for these other currents (Attwell and Cohen, 1977). The curve for slow inward current would be shifted in the same direction, but to a much smaller extent because of the smaller current densities (Fig. 6; see also Connor et al., 1975). The delayed outward current-voltage relationship would be shifted to more positive values, but also would not be affected greatly at potentials more negative than +20 mV.

The changes in membrane currents during repeated clamp steps to the same potential (Methods), which suggested an increasing series resistance, are consistent with these ideas. An increase in R_s would: (*a*) shift the inward current-voltage relationships to the left, thereby reducing the fast inward current at potentials positive to −20 mV (Fig. 6); (*b*) reduce the magnitude and kinetics of the capacitive transient, (Eq. 1); and (*c*) reduce the space constant and uniformity of potential. Similar effects have been reported in the squid giant axon as a result of uncompensated series resistance (Bezanilla et al., 1970), and have been predicted in calculations (Attwell and Cohen, 1977) and computer simulations (Ramón et al., 1975) of multicellular preparations.

The decline of damped current oscillations with repeated steps might also have been due to a progressive rise in R_s. For example, the oscillation following the fast inward transient in Fig. 1 B (R_s = 16 kΩ) may be compared with the smooth decay of I_{Na} in Fig. 2 A where series resistance was increased (R_s = 34 kΩ). These results support the hypothesis that larger values of series resistance tend to stabilize voltage-clamped preparations (Connor et al., 1975; Poindessault et al., 1976). Finally, the increase in holding current which accompanied the changes described above might have resulted not only from a progressive decline in the resistance of a leakage pathway (about the current-passing electrode) possibly aggravated by contraction, but also from an increasing

demand for current to offset the voltage drop across a rising intracellular core series resistance. In heart tissue, core resistance due to decoupling of cells undoubtedly increases as the current driven through nexal junctions exceeds a certain level (New and Trautwein, 1972). Such a reduction or block of gap junction permeability could result from leakage of extracellular calcium into the cytoplasm. This ion has been shown to increase junctional resistance between cells (Rose and Loewenstein, 1975; DeMello, 1975; Rose et al., 1977).

Current Magnitudes and Kinetics

Because it was not technically feasible to correct completely for leakage currents, most of the values we obtained for inward and outward currents are probably overestimates. Although these magnitudes were corrected for leakage at the holding potential, they may still be in error since such currents likely varied with absolute potential and may have increased during the course of voltage steps. The latter would have been true particularly of outward currents which were measured at the end of 400-ms steps.

In contrast, other factors tended to reduce the magnitudes of these currents: (*a*) the slow decay of the capacitive transient affected I_{Na}; (*b*) the activation of outward currents affected I_{si}; and (*c*) the slow inactivation of I_{si} affected outward currents. In addition, previous experiments (Nathan et al., 1976) suggest that I_{Na} is only partially activated at a holding potential of −60 mV. When membrane potential was varied with injected DC current, the maximum upstroke velocity of an action potential with maximum diastolic potential (MDP) of −60 mV was only 50% of its peak value at an MDP of −92 mV. If the maximum rate of rise is taken as a qualitative measure of availability of fast inward current (Weidmann, 1955), the maximum current density recorded for I_{Na}, −185 μA/cm^2 (Fig. 6) obtained from a holding potential of −60 mV, would be increased to ~ 370 μA/cm^2 with steps from −92 mV. These values are comparable to those obtained in adult cardiac muscle preparations where membrane surface areas have been estimated. Connor et al. (1975) recorded a peak I_{Na} in frog atrial trabeculae (from a holding potential at rest, −60 to −70 mV) of about −100 μA/cm^2, based upon electron micrographs of equivalent bundle cross sections and measurements of sucrose gap test node widths. Dudel and Rüdel (1970) obtained a maximum value of −600 μA/cm^2 (from a holding potential of −100 mV) for cooled sheep Purkinje fibers, based upon estimates of total membrane surface area from their measurements of capacitive current and an assumed value of 12 μf/cm^2 for membrane specific capacitance.

Reuter (1973) and others (Trautwein et al., 1975) have shown that in sheep ventricular trabeculae, the slow inward current is negligibly inactivated (i.e., f_∞ = 1.0) at −60 mV, and the threshold for measureable slow inward current is about −35 mV. Our current-voltage relationship for I_{si} (Fig. 6) is similar in this respect (see Fig. 7, Reuter, 1973). If we assume that I_{si} in our preparation is also negligibly inactivated at the holding potential of −60 mV, then this, in addition to the fact that delayed outward-going current was small (Fig. 2 B and Fig. 5) at the time of I_{si} measurement (10 ms), suggests that the maximum value of I_{si} (about −25 μA/cm^2) should be relatively accurate. Thus, the ratio of I_{Na}/I_{si} is between 7:1 and 14:1, depending upon the holding potential (−60 mV or −92

mV). New and Trautwein (1972) used a holding potential of −58 mV and observed a difference of ~ 10:1 for fast and slow inward currents in cat ventricular trabeculae. Chesnais et al. (1975) obtained a ratio between 8:1 and 14:1 for frog atrial trabeculae.

The kinetics of the fast inward current we recorded in embryonic heart cell aggregates, like those reported for adult cardiac muscle, were substantially slower than the analogous currents in nerve or skeletal muscle. The times at which I_{Na} and I_{si} reached their respective peaks (2.6 and 6.8 ms) as well as time constants for their decay (Fig. 3) are subject to error not only because of the slowly decaying capacitive transient and the influences of I_{si} on I_{Na}, and outward current on I_{si}, but also due to artificial shortening from a lack of complete voltage control. The fact that the times to peak current did not vary with potential further supports the latter conclusion (Connor et al., 1975). Nevertheless, time constants for the decay of I_{Na} and I_{si} (Fig. 3) are comparable to those calculated by Rougier et al. (1969) for inactivation of inward currents in frog atrial trabeculae, 1.2 ms for I_{Na} and 12 ms for I_{si}, both determined at ~ 0 mV.

The voltage dependence of time constants for slow inward current decay (Fig. 4) is similar to results obtained by New and Trautwein (1972), but their values ranged from ~ 60 ms at potentials between −25 and +10 mV to ~ 150 ms at −35 and at +40 mV. Our time constants at potentials more positive than −10 mV may have been reduced by the delayed increase in outward current at these potentials (Fig. 5 E). In addition, the values at potentials negative to −20 mV may also be in error if activation of I_{si} is slow and inactivation fast (Trautwein et al., 1975). These investigators have corrected their original curve (Trautwein et al., 1975) based upon the separation of I_{si} kinetics into activation and inactivation variables (Bassingthwaighte and Reuter, 1972). The less rapid decay of slow inward current at potentials positive to −20 mV (Fig. 4) is in qualitative agreement with results obtained from dog (Beeler and Reuter, 1970 *b*) and cow ventricular trabeculae (Reuter and Scholz, 1977).

Current-Voltage Relationships

Despite differences in current magnitudes, the shapes and thresholds of our current-voltage relationships (Fig. 6) agree relatively well with most of those determined for adult cardiac muscle (Rougier et al., 1969; Ochi, 1970; New and Trautwein, 1972; Noma and Irisawa, 1976). Nevertheless, our calculations of the effects of series resistance on I_{Na} suggest that the actual curve should be shifted to more positive potentials, possibly by as much as 20 mV. Connor et al. (1975) have demonstrated such a shift after decreasing the voltage drop across R_s by reducing the amplitude of the fast transient with TTX. Measurements from fast sweep traces of aggregate action potentials (Fig. 7 B, D), recorded just before or after voltage clamp steps, indicate that the voltage at which dV/dt of the upstroke is maximal lies between −8 and −13 mV. This agrees well with records from the dog Purkinje fiber (Draper and Weidmann, 1951) and with the reconstructed Purkinje fiber action potential (McAllister et al., 1975). To the extent that the aggregate action potential approaches a true simultaneous membrane potential (DeHaan and Fozzard, 1975), the voltage of dV/dt_{max} will roughly approximate the potential at which peak I_{Na} is achieved on the I_{Na} (V)

curve. This is another reason for suggesting that the actual value of peak I_{Na} should be somewhere between the recorded value (−20 mV, Fig. 6) and the membrane potential value (−8 to −13 mV).

Our estimates of the magnitudes and voltage dependence of I_{si} are probably fairly accurate as represented (Fig. 6). Deviation from voltage homogeneity during this slow event was < 2 mV, and the magnitude of this current, and therefore, the voltage drop across R_s was small. Thus, the existence of a slow inward current in embryonic heart cell aggregates which is independent of I_{Na} cannot be questioned on the basis of distortions of fast current due to the lack of control (Johnson and Lieberman, 1971). The following observations lend further support to this argument: (*a*) The threshold for activation of I_{si} was about −35 mV whereas that for I_{Na} was −55 mV. The uncertainty in the true membrane potential for these low current densities was < 10 mV. (*b*) The kinetics of the two currents differed by a factor between 10 and 30. (*c*) TTX selectively blocked the fast component of inward current but not the slow component (Fig. 8 C). (*d*) D600 blocked the slow component but not the fast component (Fig. 8 B). Interestingly, Lieberman et al. (1975) recorded only a single component of inward current from synthetic strands of cardiac tissue which were prepared from 11- to 13-d embryonic chick hearts. This current had a duration of about 100 ms and a voltage dependence (Fig. 4, Lieberman et al., 1975) similar to I_{si} in our 7-d aggregates. The apparent lack of a fast sodium transient in their preparation is not readily explainable.

Pharmacological Effects

Our results with TTX and D600 (Fig. 7) confirm those of McDonald and Sachs (1975) who recorded action potentials in aggregates similar to ours. The effects of these drugs upon membrane inward currents (Figs. 8 and 9) are also consistent with findings on adult cardiac tissue (Rougier et al., 1969; Besseau and Gargouïl, 1969; Kohlhardt et al., 1972; Kass and Tsien, 1975). In addition, the absence of delayed rectification in embryonic chick ventricular aggregates exposed to D600 and TTX (Fig. 9 D) agrees with results obtained in adult rat ventricular tissue (Besseau and Gargouïl, 1969). Thus, our data suggest that electrogenesis, in 7-d embryonic chick ventricle as in adult heart tissue, is based upon the sequence of a TTX-sensitive, fast transient inward current followed by a slower phase of inward current and a delayed outward current.

Summary

We have shown that with the present experimental design, spheroidal aggregates of 7-d chick ventricle cells deviate from isopotentiality, on the average, by ~ 12% during the first 3-5 ms of a voltage clamp step but approach a relatively high degree of control thereafter. Two components of inward current, and a delayed outward current, with kinetic and pharmacologic properties similar to those observed in adult cardiac tissue were recorded. With a 12% mean spatial distribution of membrane potentials and up to 50% error in the true membrane potential during the peak fast inward current due to series resistance, the actual current-voltage relationship for the fast transient would be shifted as much as

20 mV toward more positive potentials. The curves for slow inward current and for outward current are relatively accurate as illustrated.

This study confirms that spheroidal aggregates of embryonic heart cells can be used for further analyses of developmental changes in pacemaker properties and other relatively slow conductance mechanisms (Nathan and DeHaan, 1978); however, additional technical improvements will be necessary before a more accurate description of I_{Na} can be obtained.

The authors wish to thank Mrs. C. Y. Wan for her skilled technical assistance in preparing the tissue cultures, Dr. Joseph M. Kinkade for assisting with the DNA determination, and Drs. L. J. DeFelice and H. Reuter for their helpful discussion of the manuscript.

Supported in part by fellowship HL-01321 and grants HL-16567 and 17827 from the National Institutes of Health.

A preliminary report of this work was presented at the 20th Annual Meeting of the Biophysical Society held 24–27 February 1976 in Seattle, Washington [*Biophys. J.* **16**(Part 2):208*a*].

Received for publication 12 August 1977.

REFERENCES

ATTWELL, D., and I. COHEN. 1977. The voltage clamp of multicellular preparations. *Prog. Biophys. Mol. Biol.* **31**:201–245.

BASSINGTHWAIGHTE, J. B., and H. REUTER. 1972. Calcium movements and excitation-contraction coupling in cardiac cells. *In* Electrical Phenomena in the Heart. W. C. De Mello, editor. Academic Press, Inc., New York. 353–395.

BEELER, G. W., JR., and H. REUTER. 1970 *a*. Voltage clamp experiments on ventricular myocardial fibres. *J. Physiol. (Lond.).* **207**:165–190.

BEELER, G. W., JR., and H. REUTER. 1970 *b*. Membrane calcium current in ventricular myocardial fibres. *J. Physiol. (Lond.).* **207**:191–209.

BEELER, G. W., and H. REUTER. 1977. Reconstruction of the action potential of ventricular myocardial fibres. *J. Physiol. (Lond.).* **268**:177–210.

BESSEAU, A., and Y. M. GARGOUÏL. 1969. Ionic currents in rat ventricular heart fibres: voltage-clamp experiments using double sucrose-gap technique. *J. Physiol. (Lond.).* **204**: 95P–96P.

BEZANILLA, F., E. ROJAS, and R. E. TAYLOR. 1970. Sodium and potassium conductance changes during a membrane action potential. *J. Physiol. (Lond.).* **211**:729–751.

CHESNAIS, J. M., E. CORABOEUF, M. P. SAUVIAT, and J. M. VASSAS. 1975. Sensitivity to H, Li and Mg ions of the slow inward sodium current in frog atrial fibres. *J. Mol. Cell. Cardiol.* **7**:627–642.

CLAY, J. R., L. J. DEFELICE, and R. L. DEHAAN. 1978. Parameters of current noise calculated from voltage noise and impedance of the heart cell membrane near rest. *Biophys. J.* **21**:166*a*. (Abstr.)

COLE, K. S., and J. W. MOORE. 1960. Ionic current measurements in the squid giant axon membrane. *J. Gen. Physiol.* **44**:123–167.

CONNOR, J., L. BARR, and E. JAKOBSSON. 1975. Electrical characteristics of frog atrial trabeculae in the double sucrose gap. *Biophys. J.* **15**:1047–1067.

DECK, K. A., R. KERN, and W. TRAUTWEIN. 1964. Voltage clamp technique in mammalian cardiac fibres. *Pfluegers Archiv Gesamte Physiol. Menschen Tiere.* **280**:50–62.

DEFELICE, L. J., and R. L. DEHAAN. 1977. Membrane noise and intercellular communication. *Proc. IEEE.* Special Issue on Biological Signals **65**:796–799.

DEHAAN, R. L. 1967. Regulation of spontaneous activity and growth of embryonic chick heart cells in tissue culture. *Dev. Biol.* **16**:216–249.

DEHAAN, R. L. 1970. The potassium-sensitivity of isolated embryonic heart cells increases with development. *Dev. Biol.* **23**:226–240.

DEHAAN, R. L., and L. J. DEFELICE. 1978. Oscillatory properties and excitability of the heart cell membrane. *In* Theoretical Chemistry: Advances and Perspectives. H. Eyring, editor. Academic Press, Inc., New York. **4**:181–233.

DEHAAN, R. L., and H. A. FOZZARD. 1975. Membrane response to current pulses in spheroidal aggregates of embryonic heart cells. *J. Gen. Physiol.* **65**:207–222.

DEHEMPTINNE, A. 1976. Voltage clamp analysis in isolated cardiac fibres as performed with two different perfusion chambres for double sucrose gap. *Pfluegers Arch. Eur. J. Physiol.* **363**:87–95.

DEMELLO, W. C. 1975. Effect of intracellular injection of calcium and strontium on cell communication in heart. *J. Physiol. (Lond.).* **250**:231–245.

DRAPER, M. H., and S. WEIDMANN. 1951. Cardiac resting and action potentials recorded with an intracellular electrode. *J. Physiol. (Lond.).* **115**:74–94.

DUDEL, J., and R. RUDEL. 1970. Voltage and time dependence of excitatory sodium current in cooled sheep Purkinje fibres. *Pfluegers Arch. Eur. J. Physiol.* **315**:136–158.

ELSAS, L. J., F. B. WHEELER, D. J. DANNER, and R. L. DEHAAN. 1975. Amino acid transport by aggregates of cultured chicken heart cells: effect of insulin. *J. Biol. Chem.* **250**:9381–9390.

FOZZARD, H. A., and G. W. BEELER, JR. 1975. The voltage clamp and cardiac electrophysiology. *Circ. Res.* **37**:403–413.

GILES, K. W., and A. MYERS. 1965. An improved diphenylamine method for the estimation of deoxyribonucleic acid. *Nature (Lond.).* **206**:93.

GOLDMAN, Y., and M. MORAD. 1977. Measurement of transmembrane potential and current in cardiac muscle: a new voltage clamp method. *J. Physiol. (Lond.).* **268**:613–654.

HAAS, H. G., R. KERN, H. M. EINWÄCHTER, and M. TARR. 1971. Kinetics of Na inactivation in frog atria. *Pfluegers Arch. Eur. J. Physiol.* **323**:141–157.

HECHT, H. H., O. F. HUTTER, and D. W. LYWOOD. 1964. Voltage-current relation of short Purkinje fibres in sodium-deficient solution. *J. Physiol. (Lond.).* **170**:5P–7P.

HELLAM, D. C., and J. W. STUDT. 1974. Core conductor model of cardiac Purkinje fiber based on structural analysis. J. Physiol. (*Lond.*). **243**:637–660.

HIRAKOW, R., and T. GOTOH. 1975. A quantitative ultrastructural study on the developing rat heart. *In* Developmental and Physiological Correlates of Cardiac Muscle. M. Lieberman and T. Sano, editors. Raven Press, New York. 37–49.

ISHIMA, Y. 1968. Changes in properties of the excitable membrane of the embryonic chicken heart during the course of its development. *Proc. Jpn. Acad.* **44**:170–178.

JOHNSON, E. A., and M. LIEBERMAN. 1971. Heart: Excitation and contraction. *Annu. Rev. Physiol.* **33**:479–532.

KASS, R. S., and R. W. TSIEN. 1975. Multiple effects of calcium antagonists on plateau currents in cardiac Purkinje fibers. *J. Gen. Physiol.* **66**:169–192.

KENSLER, R. W., P. BRINK, and M. M. DEWEY. 1977. Nexus of frog ventricle. *J. Cell Biol.* **73**:768–782.

KOHLHARDT, M., B. BAUER, H. KRAUSE, and A. FLECKENSTEIN. 1972. Differentiation of the transmembrane Na and Ca channels in mammalian cardiac fibres by the use of specific inhibitors. *Pfluegers Arch. Eur. J. Physiol.* **335**:309–322.

LIEBERMAN, M., T. SAWANOBORI, N. SHIGETO, and E. A. JOHNSON. 1975. Physiologic

implications of heart muscle in tissue culture. *In* Developmental and Physiological Correlates of Cardiac Muscle. M. Lieberman and T. Sano, editors. Raven Press, New York. 139–154.

MCALLISTER, R. E., D. NOBLE, and R. W. TSIEN. 1975. Reconstruction of the electrical activity of cardiac Purkinje fibres. *J. Physiol. (Lond.).* **251:**1–59.

MCDONALD, T. F., and R. L. DEHAAN. 1973. Ion levels and membrane potential in chick heart tissue and cultured cells. *J. Gen. Physiol.* **61:**89–109.

MCDONALD, T. F., and H. G. SACHS. 1975. Electrical activity in embryonic heart cell aggregates: Developmental aspects. *Pfluegers Arch. Eur. J. Physiol.* **354:**151–164.

MCDONALD, T. F., H. G. SACHS, and R. L. DEHAAN. 1972. Development of sensitivity to tetrodotoxin in beating chick embryo hearts, single cells, and aggregates. *Science (Wash. D.C.).* **176:**1248–1250.

MCGUIGAN, J. A. S. 1974. Some limitations of the double sucrose gap, and its use in a study of the slow outward current in mammalian ventricular muscle. *J. Physiol. (Lond.).* **240:**775–806.

MOOLENAAR, W. H., and I. SPECTOR. 1978. Ionic currents in cultured mouse neuroblastoma cells under voltage clamp conditions. *J. Physiol. (Lond.).* **278:**265–286.

NARAHASHI, T. 1974. Chemicals as tools in the study of excitable membranes. *Physiol. Rev.* **54:**813–889.

NATHAN, R. D., and R. L. DEHAAN. 1978. In vitro differentiation of a fast Na^+ conductance in embryonic heart cell aggregates. *Proc. Natl. Acad. Sci. U. S. A.* **75:**2776–2780.

NATHAN, R. D., J. P. POOLER, and R. L. DEHAAN. 1976. Ultraviolet-induced alterations of beat rate and electrical properties of embryonic chick heart cell aggregates. *J. Gen. Physiol.* **67:**27–44.

NEW, W., and W. TRAUTWEIN. 1972. Inward membrane currents in mammalian myocardium. *Pfluegers Arch. Eur. J. Physiol.* **334:**1–23.

NOMA, A., and H. IRISAWA. 1976. Membrane currents in the rabbit sinoatrial node cell as studied by the double microelectrode method. *Pfluegers Arch. Eur. J. Physiol.* **364:**45–52.

OCHI, R. 1970. The slow inward current and the action of manganese ions in guinea-pig's myocardium. *Pfluegers Arch. Eur. J. Physiol.* **316:**81–94.

POINDESSAULT, J. P., A. DUVAL, and C. LÉOTY. 1976. Voltage clamp with double sucrose gap technique: External series resistance compensation. *Biophys. J.* **16:**105–120.

RAMÓN, F., N. ANDERSON, R. W. JOYNER, and J. W. MOORE. 1975. Axon voltage-clamp simulations. IV. A multicellular preparation. *Biophys. J.* **15:**55–69.

REUTER, H. 1973. Divalent cations as charge carriers in excitable membranes. *Prog. Biophys. Mol. Biol.* **26:**1–43.

REUTER, H., and H. SCHOLZ. 1977. A study of the ion selectivity and the kinetic properties of the calcium dependent slow inward current in mammalian cardiac muscle. *J. Physiol. (Lond.).* **264:**17–47.

ROSE, B., and W. R. LOEWENSTEIN. 1975. Permeability of cell junction depends on local cytoplasmic calcium activity. *Nature (Lond.).* **254:**250–252.

ROSE, B., I. SIMPSON, and W. R. LOEWENSTEIN. 1977. Calcium ion produces graded changes in permeability of membrane channels in cell junction. *Nature (Lond.).* **267:**625–627.

ROUGIER, O., G. VASSORT, D. GARNIER, Y. M. GARGOUÏL, and E. CORABOEUF. 1969. Existence and role of a slow inward current during the frog atrial action potential. *Pfluegers Arch. Eur. J. Physiol.* **308:**91–110.

SACHS, H. G., and R. L. DEHAAN. 1973. Embryonic myocardial cell aggregates: Volume and pulsation rate. *Dev. Biol.* **30**:233–240.

SACHS, H. G., T. F. MCDONALD, and M. SPRINGER. 1974. Cytochalasin B and embryonic heart muscle: contractility, excitability and ultrastructure. *J. Cell Sci.* **14**:163–185.

SANTORA, A. C., F. B. WHEELER, R. L. DEHAAN, and L. J. ELSAS. 1978. Relationship of insulin binding to amino acid transport by cultured 14-day embryonic chick heart cells. *Endocrinology*. In press.

SHIGENOBU, K., J. A. SCHNEIDER, and N. SPERELAKIS. 1974. Verapamil blockade of slow Na^+ and Ca^{++} responses in myocardial cells. *J. Pharmacol. Exp. Ther.* **190**:280–288.

SHIGENOBU, K., and N. SPERELAKIS. 1971. Development of sensitivity to tetrodotoxin of chick embryonic hearts with age. *J. Mol. Cell. Cardiol.* **3**:271–286.

TARR, M., and J. W. TRANK. 1974. An assessment of the double sucrose-gap voltage clamp technique as applied to frog atrial muscle. *Biophys. J.* **14**:627–643.

TASAKI, K., Y. TSUKAHARA, and S. ITO. 1968. A simple, direct and rapid method for filling microelectrodes. *Physiol. Behav.* **3**:1009–1010.

TRAUTWEIN, W. 1973. Membrane currents in cardiac muscle fibers. *Physiol. Rev.* **53**:793–835.

TRAUTWEIN, W., and T. F. MCDONALD. 1978. Membrane conductance measurements in cat ventricular muscle. *J. Mol. Cell. Cardiol.* **10**:387–394.

TRAUTWEIN, W., T. F. MCDONALD, and O. TRIPATHI. 1975. Calcium conductance and tension in mammalian ventricular muscle. *Pfluegers Arch. Eur. J. Physiol.* **354**:55–74.

WEIDMANN, S. 1955. The effect of the cardiac membrane potential on the rapid availability of the sodium-carrying system. *J. Physiol. (Lond.)*. **127**:213–224.